Synergistic effect of hyperosmotic agents and sonophoresis on breast tissue optical properties and permeability studied with spectral domain optical coherence tomography

Zhenguo Zhu
Huajiang Wei
Guoyong Wu
Hongqin Yang
Yonghong He
Shusen Xie

Synergistic effect of hyperosmotic agents and sonophoresis on breast tissue optical properties and permeability studied with spectral domain optical coherence tomography

Zhenguo Zhu,[a] Huajiang Wei,[a] Guoyong Wu,[b] Hongqin Yang,[c] Yonghong He,[d] and Shusen Xie[c]
[a]South China Normal University, College of Biophotonics, MOE Key Laboratory of Laser Life Science & Institute of Laser Life Science, Guangzhou 510631, China
[b]Sun Yat-Sen University, The First Affiliated Hospital, Department of Surgery, Guangzhou 510080, Guangdong, China
[c]Fujian Normal University, Key Laboratory of Optoelectronic Science and Technology for Medicine of Ministry of Education of China, Fuzhou 350007, Fujian, China
[d]Tsinghua University, Graduate School at Shenzhen, Shenzhen 518055, Guangdong, China

Abstract. Hyperosmotic agents have shown great potential in tissue optical clearing. However, the low efficiency of the permeation in biological tissues seriously restricts its application in reality. The synergy of sonophoresis as a penetration enhancer and hyperosmotic agents, 20% glucose (G) and 20% mannitol (M), in optical clearing has been investigated by analyzing the variation of the attenuation coefficients and the permeability coefficients. In the sonophoresis experiments, ultrasound (US) was applied for 10 min before applying hyperosmotic agents. Along with the administration of hyperosmotic agents, the samples were monitored with optical coherence tomography (OCT) functional imaging for the next 2 h. The attenuation coefficients of each group were obtained from the 2-D OCT images based on Beer's Law. The original attenuation coefficient is 12.38 ± 0.73 cm^{-1} in normal breast tissue. After 45 min treatment, it changes to be 5.91 ± 0.82 cm^{-1} and 4.14 ± 0.67 cm^{-1} for 20% G and 20% G/US, respectively. The attenuation coefficient of breast cancer tissue is 18.17 ± 1.45 cm^{-1} at the beginning, and it becomes 8.70 ± 0.87 cm^{-1} for 20% G and 6.80 ± 0.92 cm^{-1} for 20% G/US after 30 min. Meanwhile, the permeability coefficients of hyperosmotic agents were much enlarged by the treatment of ultrasound in both breast normal tissue and breast cancer tissue. A significant difference in permeability coefficients between health tissue and tumor tissue was also observed in the experiment ($p < 0.01$). © 2012 Society of Photo-Optical Instrumentation Engineers (SPIE). [DOI: 10.1117/1.JBO.17.8.086002]

1 Introduction

Tissue optics has been widely utilized in laser-based therapeutic and diagnostic techniques.[1–5] However, the turbidity of biological tissues, which imposes limitation on light penetration depth, has severely affected its biomedical application. Recent progress in engineered tissue optics provides a useful means to enhance light penetration into turbid tissues, which allows reversibly altering the light scattering and absorption properties of turbid biological tissues in a controllable manner.[6–9] This approach, for example, leads to enhanced signal detection in optical coherence tomography (OCT).[10] Tissue optical clearing, which uses hyperosmotic agents [optical clearing agents (OCA)] to modify biological tissue's scattering property and refractive index, holds great promise in reducing light scattering in turbid biological tissues and enhancing optical penetration depth.[11–14] Three hypothesized mechanisms of tissue optical clearing induced by hyperosmotic agents have been proposed: (1) dehydration of tissue constituents; (2) partial replacement of the interstitial fluid by the immersion substance; and (3) structural modification or dissociation of structured proteins, such as collagen.[7,8,15–17]

The first and second mechanisms are supposed to be the primary factors that contribute to the refractive indices' match of tissue components.

OCT, as an advanced high-resolution structural imaging technology based on low coherence interferometry, has shown great promise in noninvasive real-time diagnosis.[18–20] Breast cancer is the most frequently diagnosed cancer and the leading cause of cancer death in females worldwide, according to 1.38 million new cancer cases and 4,58,400 deaths in 2008.[21,22] A noninvasive and effective diagnostic technique is urged for early breast cancer detection and OCT technology can be the possible means. Because of the pathological changes of cancer tissue's morphology and structure, the diversity of permeability and optical property occurs between normal tissue and cancerous tissue. Based on the differences in permeability and optical property, OCT technology can be used to distinguish cancerous tissues from normal tissues. This method has been demonstrated by previous studies,[23–25] and has also been applied for breast cancer detection.[26,27]

Glucose (G) is one of the most commonly used OCAs which have been widely used to investigating the permeability of biological tissues. Mannitol (M) is a hyperosmotic agent with similar molecular weight to glucose. The optical clearing

---

Address all correspondence to: Huajiang Wei, South China Normal University, College of Biophotonics, MOE Key Laboratory of Laser Life Science & Institute of Laser Life Science, Guangzhou 510631, Guangdong, China. Tel: +86-20-85217070-8603; Fax: +86-20-85216052; E-mail: weihj@scnu.edu.cn

efficacy and the potential in cancer diagnostic of these agents have been investigated in our previous study.[27] However, the low permeation efficiency of hyperosmotic agents in biological tissues limits its practical implementation. To improve the permeability of biological tissues, a number of different chemical and physical methods have been proposed, such as chemical enhancer,[28] electroporation,[29] iontophoresis,[30] microneedle,[31] sonophoresis (ultrasound),[32] etc. Despite the widespread use of ultrasound (US) in transdermal drug delivery (TDD), there are few studies to apply ultrasound on inner tissue optical clearing. Recently, Zhong et al. reported that sonophoresis, as a noninvasive physical method, exhibited an enhancing breast tissue clearing effect when applied with glycerol and the results indicated that this method was feasible.[33] The application of ultrasound can result in cavitation, thermal and mechanical effects in biological tissues, and thus enhances the permeation of OCA.[34] Nevertheless, more studies are needed to make sure of the synergistic effect of ultrasound with hyperosmotic agents in different tissues, which will contribute to finding an optimal OCA and make optical clearing technique more practical.

In order to find a more efficient way to enhance the diffusion of glucose and mannitol in inner tissues, we investigated the optical clearing efficacy of 20% G and 20% M in human breast cancer tissue (BC) and normal breast tissue (NB) *in vitro* with the synergistic treatment of ultrasound. The diffusion process of the agents in breast cancer tissue and normal breast tissue were monitored with a spectral domain OCT during the experiment. This research may improve the capability of OCT utilized in cancer detection and help patients with breast cancer by providing prompt diagnosis.

2 Materials and Methods

2.1 Experimental Setup

The experiments were performed with a spectral domain OCT system (SD-OCT). The optical source used in this system is a low-coherence broadband super luminescent diode with a wavelength of 830 ± 40 nm and an output power of 5 mW. The SD-OCT system provides an axial resolution of 12 μm and a transverse resolution of 15 μm in free space, determined by the focal spot size of the probe beam. The signal-to-noise ratio of the OCT system is measured to be 120 dB. Two-dimensional (2-D) images are obtained by scanning the incident beam over the sample surface in the lateral direction and in-depth (A-scan) scanning by the interferometer. The acquisition time per OCT image is about 180 ms, corresponding to an A-scan frequency of 2000 Hz. A computer is used to control the OCT system with a data acquisition software written in Lab View 7.2-D. OCT images obtained in the experiment were stored in the computer for further processing.

In this experiment, a sonicator (DM-F608, Dimyth Beauty Equipment Manufacture, Guangzhou, China) with a frequency of about 1 MHz and an intensity of 0.8 W/cm^2 was used for ultrasound application. Sonicator with this frequency is usually used for cosmetic treatments and TDD. In order to avoid any thermal effect, a transducer with a diameter of about 0.8 cm was used with a pulsed mode (500 ms pulses applied every second). During sonication, the ultrasound probe was immersed in the topical applied physiological saline with sufficient contact pressure. The temperature of the specimens was measured periodically with a thermocouple (Digithermo, VWR Scientific,

Table 1 Groups and treatment in this experiment.

Groups	Normal breast tissue	Groups	Breast cancer tissue
1	20% G	5	20% G
2	20% G/US	6	20% G/US
3	20% M	7	20% M
4	20% M/US	8	20% M/US

PA, USA). No significant increase in temperature ($<2°C$) was observed during ultrasound exposure.

2.2 Samples and Agents

Excised surgical specimens were collected from ten female patients. All the breast tissues were stored in a refrigerator at $-70°C$ until measurement. During the experiment, histology samples were grouped into two critical cases: normal breast tissues and ductal carcinoma (the most common breast cancer) tissues. Before experiment, glucose and mannitol solution with the same concentration of 20% (w/v) were prepared using standard method. The materials with lateral dimension of approximately 1.2×1.2 cm^2 were prepared in freezing state. All the samples were divided into eight groups, as showed in Table 1, and each group contain six specimens. At the beginning, samples were unfrozen in physiological saline at room temperature for 30 min. In order to get a baseline, the selected region of each sample was monitored about 8 to 10 min by OCT system before applying hyperosmotic agents and ultrasound. In the sonophoresis experiments, ultrasound was applied for 10 min at each sample before surface applying hyperosmotic agents. With the administration of hyperosmotic agents, the samples were immediately monitored with 2-D OCT functional imaging for the next 2 h at 22°C. Each sample was used only once.

2.3 Methods

In order to characterize the changes of optical properties in the breast tissues during the experiment, the attenuation coefficients of each group were calculated from the 2-D OCT image, as it carries the information of the reflected light intensity distribution in depth of the tissue. The reflected light intensity depends on the tissue's optical property, i.e., the absorption coefficient (μ_a) and scattering coefficient (μ_s), or called total attenuation coefficient (μ_t) which equals the sum of scattering coefficient (μ_s), and absorption coefficient (μ_a). For collimated light propagation in relatively transparent tissues, it is assumed that the reflected light intensity distribution follows Beer's Law where

$$I = I_0 \times e^{-(\mu_t \cdot L)}, \quad (1)$$

with I is the light intensity at the depth L from tissue surface and I_0 is the incident light intensity, and L the depth from tissue surface. In the OCT system case, Eq. (1) is transformed to be[35,36]

$$I_2 = I_1 \times e^{-(2\mu_t \cdot \Delta L)}, \quad (2)$$

where $\Delta L = |L_2 - L_1|$, I_1 and I_2 are the reflected light intensity at the selected depth L_1 and L_2, respectively. The factor of two in the exponential accounts for the light passing through the tissue twice after being backscattered. Therefore, μ_t can be obtained theoretically from the OCT signal intensity measurements at two different depths:

$$\mu_t = \frac{1}{2 \times \Delta L} \ln\left(\frac{I_1}{I_2}\right). \tag{3}$$

An averaged optical intensity profile that represents the reflected light intensity distribution in depth is obtained by averaging the 2-D image laterally over 1 mm, which is wide enough for speckle noise suppression. As noise is inevitable in the measurement, a best-fit exponential curve is applied to the averaged intensity profiles of each group.

The permeability coefficients of hyperosmotic agents in the breast tissue were calculated with the OCT signal slope (OCTSS) method.[37,38] The permeability coefficient is obtained by analyzing the changes of OCTSS in a selected region during the diffusion process of hyperosmotic agents. A linear region with minimal fluctuation in the averaged OCT signal profile is selected and its physical thickness (ΔL) is measured (assuming the refractive index of 1.4). The OCTSS of the linear region for each image is computed with a Matlab program. The increasing concentration

of hyperosmotic agents in the selected region induces the decrease of the scattering, which is clearly reflected in the OCTSS graph. The diffusion time (Δt) is measured from the point where the OCTSS started to decrease to the point at which a reverse process takes place. The permeability coefficient (P) is calculated by dividing the thickness of the linear region (ΔL) by the diffusion time (Δt):[37]

$$P = \frac{\Delta L}{\Delta t}. \tag{4}$$

2.4 Statistical Analysis

The data were presented as a mean $\pm$ SD for a number of samples. Statistical analyses were performed by Student's t-tests with the statistics software SPSS 13.0. $P < 0.05$ was considered statistically significant.

3 Result and Discussion

Continuous monitoring of the tissues during the 2 h permeation experiments were performed by 2-D OCT imaging for each group. With the same condition and procedure, six independent experiments were carried out for each group. Figures 1(a) and 2(a) are the typical OCT images of normal breast tissue and breast cancer tissue, respectively. Figures 1(b) and 2(b)
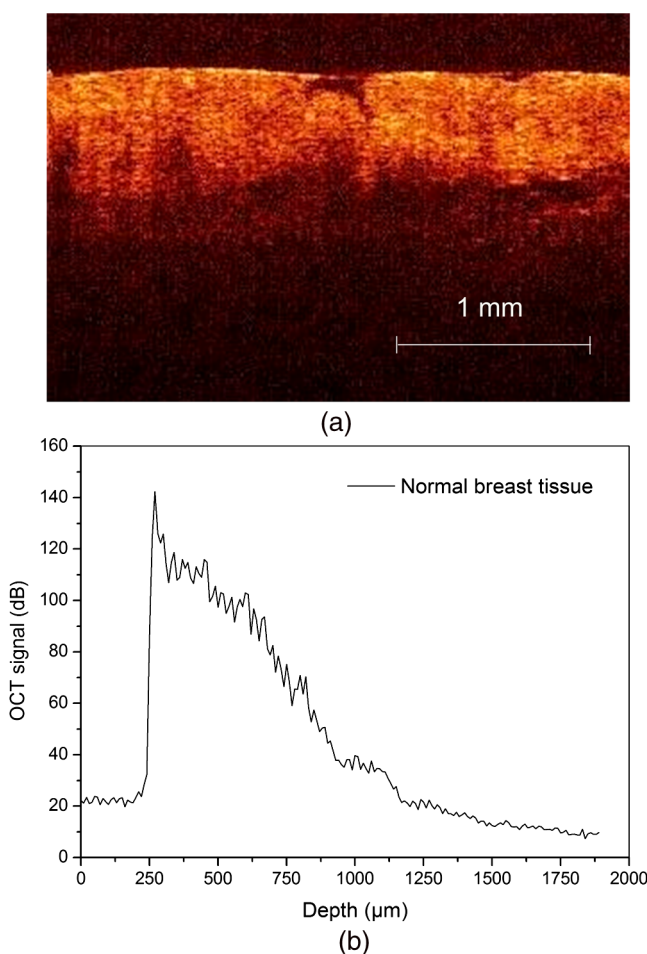

Fig. 1 (a) The typical OCT image of normal breast tissue and (b) the averaged OCT signal profile versus depth extracted from the selected region in OCT image (a).
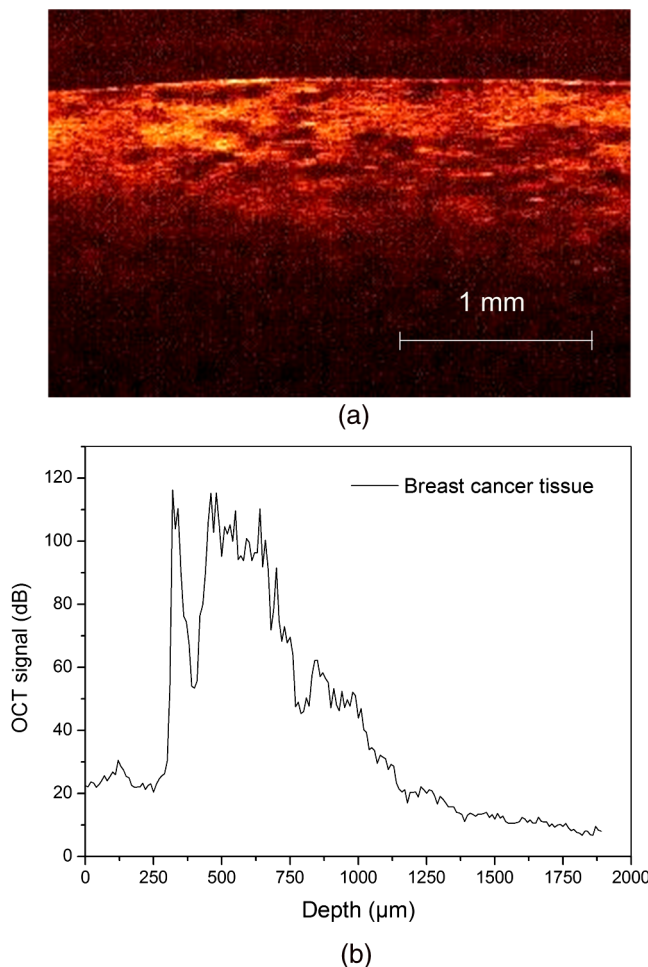

Fig. 2 (a) The typical OCT image of breast cancer tissue and (b) the averaged OCT signal profile versus depth extracted from the selected region in OCT image (a).

are the averaged intensity profiles extracted from Figs. 1(a) and 2(a). By analyzing Figs. 1 and 2, it is obvious that the structure of normal breast tissue is more homogeneous than that of breast cancer tissue. Besides, the OCT signal intensity in breast cancer tissue is about 10 percent lower than that in normal breast tissue. It means that the scattering in the tumor tissue is stronger than that in normal breast tissue. The difference in optical property between normal breast tissue and breast cancer tissue may be induced by the morphological and structural differences between the two types of tissues, such as larger nuclei, the higher nuclear-to-cytoplasmic ratio in tumor cells, and the higher regional tumor cell density of the tumor tissues.[23]

The attenuation coefficients of each group at different time were calculated from the data of the best exponential fit curve corresponding to the averaged intensity profiles. The selected region is from the depth of 110 μm (L_1) to the depth of 280 μm (L_2), where the OCT signal distribution is relatively smooth. Figure 3 presents the attenuation coefficients of normal breast tissue at 0, 5, 15, 30, 45, and 60 min after topical applying 20% G, in which the magenta bar stand for the ultrasound treated group and the yellow bar represent untreated group. Figure 4 shows the changes of the attenuation coefficients in breast cancer tissue treated with 20% G and 20% G/US, respectively. The attenuation coefficients of normal breast tissue are 12.38± 0.73 cm^{-1} for 20% G and 12.26 ± 0.79 cm^{-1} for 20% G/US at 0 min, but it changed to be 5.91 ± 0.82 cm^{-1} for 20% G and 4.14 ± 0.67 cm^{-1} for 20% G/US at 45 min when the diffusion process reached the stable state. As to breast cancer tissue, the attenuation coefficients are 18.17 ± 1.45 cm^{-1} for 20% G and 18.54 ± 0.98 cm^{-1} for 20% G/US at 0 min, while at 30 min, it is 8.70 ± 0.87 cm^{-1} for 20% G and 6.80 ± 0.92 cm^{-1} for 20% G/US. By analyzing these data, it is obvious that the attenuation coefficients in the same kind of breast tissues are almost equal at the beginning no matter whether treated with ultrasound or not ($p > 0.05$). However, a significant difference in the attenuation coefficients occurs between the groups treated with ultrasound and that without during the agents' diffusing process ($p < 0.05$). The attenuation coefficient was reduced by about 52% in normal breast tissue after 45 min treatment of 20% G; while with the
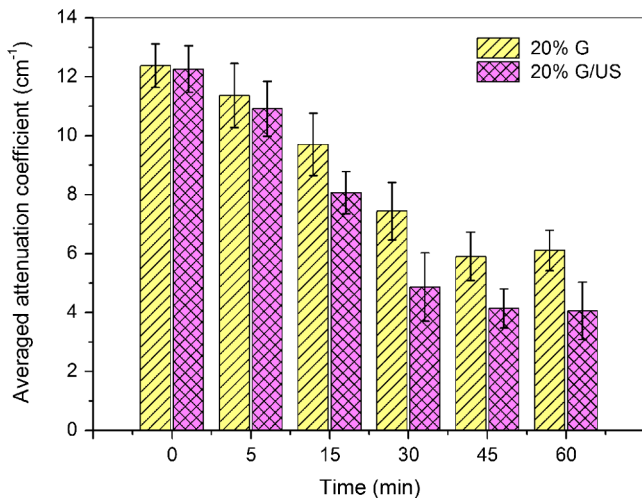

Fig. 4 The attenuation coefficients of breast cancer tissue at 0, 5, 10, 20, 30 and 45 min after topical applying 20% glucose, in which the yellow bar represent the control group and the magenta bar stand for the ultrasound treated group.

(a)

(b)

Fig. 3 The attenuation coefficients of normal breast tissue at 0, 5, 15, 30, 45 and 60 min after topical applying 20%G, in which the yellow bar represent the control group and the magenta bar stand for the ultrasound treated group.
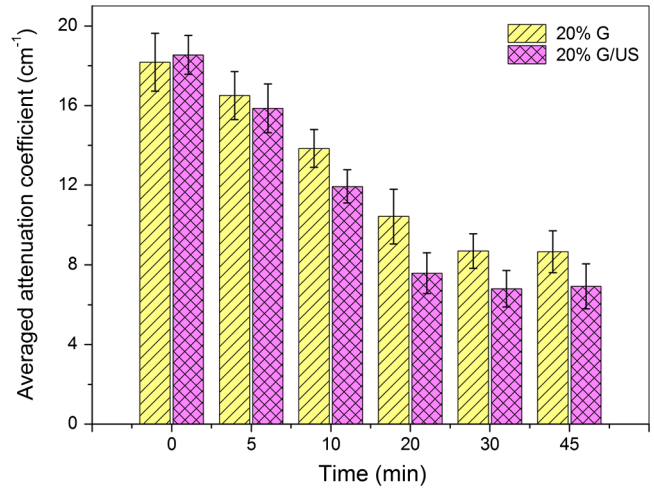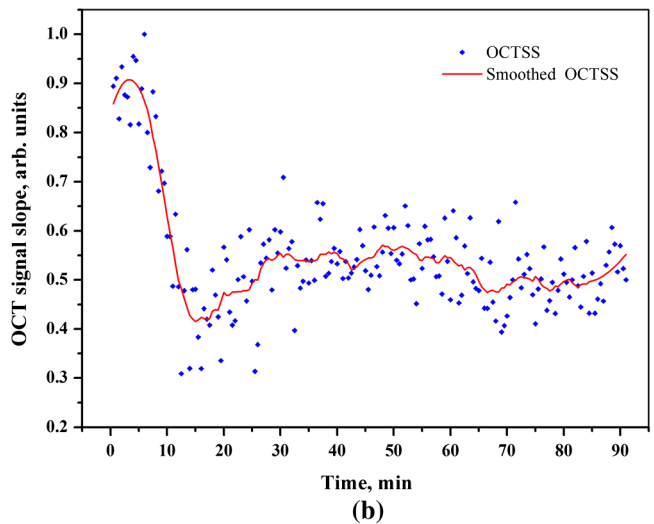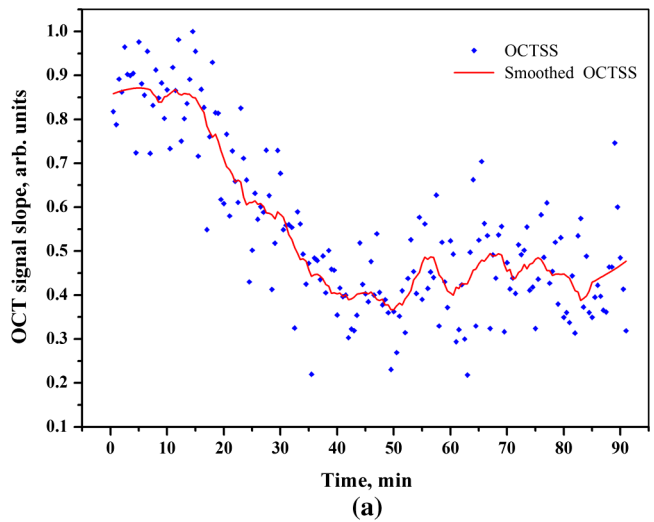
Fig. 5 OCT signal slope as a function of time recorded from (a) normal breast tissue and (b) cancerous tissue during 20% glucose diffusion process, both with the treatment of ultrasound.

treatment of 20% G/US, the attenuation coefficient was decreased by approximately 66%. The similar result was also observed in skin tissue.[39] This phenomenon could be induced by the cavitation effect of ultrasound, which has been demonstrated in TDD experiments.[34] This effect not only makes biological tissues more permeable but also promotes more hyperosmotic agents penetrating into tissues. Therefore, the refractive indices of the tissue components match better, which reflects in a low attenuation coefficient. Ultrasound has shown the similar effect as a penetration enhancer in the 20% M penetration experiment whose data are not shown. The results have demonstrated that ultrasound has a positive effect on the optical clearing of tissues, and there is a significant difference in the attenuation coefficients between normal breast tissue and tumor tissue ($p < 0.01$).

For further study of the effect of ultrasound as an important penetration enhancer, the permeability coefficient, as an important parameter for tissue optical clearing, was also calculated using OCTSS method. The OCTSS was calculated in the range of about 200 μm at depth of approximately 150 μm away from the tissue surface. Figures 5 and 6 present the changes of OCTSS over time for breast tissues treated with

Table 2 The permeability coefficient of each group for breast tissues.

Treatment	Permeability coefficient ($\times 10^{-6}$ cm/s)	
	Normal breast tissue	Breast cancer tissue
20% G	8.55 ± 1.64	19.31 ± 1.76
20% G/US	12.63 ± 1.35	28.79 ± 2.38
20% M	7.05 ± 1.17	13.88 ± 1.91
20% M/US	9.81 ± 1.48	22.15 ± 1.82

20% G/US and 20% M/US, respectively. The OCTSS decreased prominently during the diffusion process after the treatment of ultrasound. The decreasing of the OCTSS means that more photons get into the tissues and the scattering inside the tissues is reduced with the diffusion of the agents. In Fig. 5(a), glucose solution reached the monitored region at approximately 12 min after treated with ultrasound and took another 28 min for it to complete diffusion in normal breast tissues; while it only took 11 min to completely diffuse though the whole region for the breast cancer tissues with the same condition [Fig. 5(b)]. Although both being treated with ultrasound, the diffusion of 20% M in the breast cancer tissue just used about 16 min to diffuse through the selected region, while it took about 34 min in normal breast tissue. Consequently, the diffusion process in breast cancer tissue is much faster than that in normal breast tissue, which is consistent well with our former studies.[26,27]

The permeability coefficients of all groups are shown in Table 2. The results of this study indicated that the permeability coefficient of hyperosmotic agents in the same kind of breast tissues after treating with ultrasound is larger than that without ultrasound ($p < 0.01$). The permeability coefficient of 20% M in normal breast tissues was enlarged 36% by ultrasound; and in breast cancer tissue, ultrasound has enlarged the permeability of 20% M by about 59%. Compared with the permeability coefficients of the breast tissue without ultrasound, which has been present in our previous study,[27] one can conclude that the agents' diffusion process has been dramatically accelerated by the sonophoresis. This is consistent with the previous findings that ultrasound can improve the permeability of biological tissues.[40–42] Moreover, there is a significant difference in permeability coefficients between breast cancer tissues and normal breast tissues with the same treatment ($p < 0.01$).

4 Conclusion

In this study, we have demonstrated the efficacy of glucose and mannitol in low concentration as OCA in breast tissues. In addition, the results indicates that there is a dramatic difference in optical property between normal breast tissue and breast cancer tissue. Due to the difference in structure and morphology, the attenuation coefficient in breast cancer tissues is larger than that in normal breast tissues. Most importantly, we have done particular research on the influence of ultrasound to the diffusion process as an important penetration enhancer. Results suggest that sonophoresis can accelerate the diffusion process of hyperosmotic agents and improve the effect of optical clearing. Therefore, it has a potential to become a useful tool for the enhancement of tissues' permeability and optical clearing.
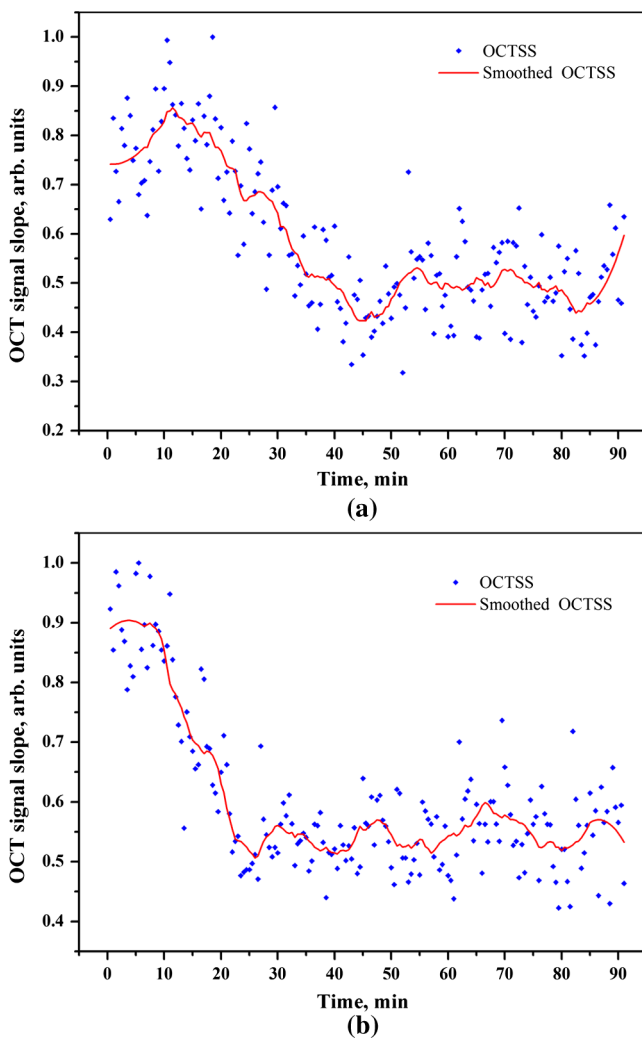

Fig. 6 OCT signal slope as a function of time recorded from (a) normal breast tissue and (b) cancerous tissue during 20% mannitol diffusion process, both with the treatment of ultrasound.

References

1. L. T. Perelman, "Optical diagnostic technology based on light scattering spectroscopy for early cancer detection," *Expert Rev. Med. Devices* **3**(6), 787–803 (2006).

2. S. A. Boppart et al., "Intraoperative assessment of microsurgery with three-dimensional optical coherence tomography," *Radiology* **208**(1), 81–86 (1998).

3. R. L. P. van Veen et al., "Intraoperatively assessed optical properties of malignant and healthy breast tissue used to determine the optimum wavelength of contrast for optical mammography," *J. Biomed. Opt.* **9**(6), 1129–1136 (2004).

4. K. Sokolov et al., "Polarized reflectance spectroscopy for pre-cancer detection," *Technol. Cancer Res. Treat.* **3**(1), 1–14 (2004).

5. N. Agrawal et al., "Wavelet transform of breast tissue fluorescence spectra—a technique for diagnosis of tumors," *IEEE J. Sel. Top. Quantum Electron.* **9**(2), 154–161 (2003).

6. V. V. Tuchin et al., "Light propagation in tissues with controlled optical properties," *Proc. SPIE* **2925**, 118–142 (1996).

7. A. T. Yeh et al., "Reversible dissociation of collagen in tissues," *J. Invest. Dermatol.* **121**, 1332–1335 (2003).

8. A. T. Yeh and J. Hirshburg, "Molecular interactions of exogenous chemical agents with collagen—implications for tissue optical clearing," *J. Biomed. Opt.* **11**(1), 014003 (2006).

9. E. A. Genina, A. N. Bashkatov, and V. V. Tuchin, "Tissue optical immersion clearing," *Expert Rev. Med. Devices.* **7**(6), 825–842 (2010).

10. R. K. Wang, "Tissue clearing as a tool to enhance imaging capability for optical coherence tomography," *Proc. SPIE* **4619**, 22–25 (2002).

11. V. V. Tuchin, "Optical clearing of tissue and blood using immersion method," *J. Phys. D* **38**(15), 2497–2518 (2005).

12. J. Jiang et al., "Penetration kinetics of dimethyl sulphoxide and glycerol in dynamic optical clearing of porcine skin tissue in vitro studied by Fourier transform infrared spectroscopic imaging," *J. Biomed. Opt.* **13**(2), 021105 (2008).

13. R. V. Kuranov et al., "In vivo study of glucose-induced changes in skin properties assessed with optical coherence tomography," *Phys. Med. Biol.* **51**(16), 3885–3900 (2006).

14. I. V. Larina et al., "Enhanced OCT imaging of embryonic tissue with optical clearing," *Laser Phys. Lett.* **5**(6), 476–479 (2008).

15. C. G. Rylander et al., "Dehydration mechanism of optical clearing in tissue," *J. Biomed. Opt.* **11**(4), 041117 (2006).

16. R. K. Wang, "Role of mass diffusion and water desorption on optical clearing of biological tissue immersed with the hyperosmotic agents," *Proc. SPIE* **5330**, 160–166 (2004).

17. J. Hirshburg et al., "Collagen solubility correlates with skin optical clearing," *J. Biomed. Opt.* **11**(4), 040501–040503 (2006).

18. A. M. Sergeev et al., "In vivo endoscopic OCT imaging of precancer and cancer states of human mucosa," *Opt. Express* **1**(13), 432–440 (1997).

19. N. V. Iftimia et al., "Spectral-domain low coherence interferometry/optical coherence tomography system for fine needle breast biopsy guidance," *Rev. Sci. Instrum.* **80**(2), 024302 (2009).

20. P. H. Tomlins and R. K. Wang, "Theory, developments and applications of optical coherence tomography," *J. Phys. D Appl. Phys.* **38**(15), 2519 (2005).

21. A. Jemal et al., "Global cancer statistics," *CA Cancer J. Clin.* **61**(2), 69–90 (2011).

22. J. Ferlay et al., "Estimates of worldwide burden of cancer in 2008: GLOBOCAN 2008," *Int. J. Cancer* **127**(12), 2893–2917 (2010).

23. M. G. Ghosn et al., "Permeability of hyperosmotic agent in normal and atherosclerotic vascular tissues," *J. Biomed. Opt.* **13**(1), 010505 (2008).

24. Q. L. Zhao et al., "Quantifying glucose permeability and enhanced light penetration in ex vivo human normal and cancerous esophagus tissues with optical coherence tomography," *Laser Phys. Lett.* **8**(1), 71–77 (2011).

25. X. Guo et al., "Quantification of glucose diffusion in human lung tissues by using Fourier domain optical coherence tomography," *Photochem. Photobiol.* **88**(2), 311–316 (2012).

26. H. Q. Zhong et al., "Quantification of glycerol diffusion in human normal and cancer breast tissues in vitro with optical coherence tomography," *Laser Phys. Lett.* **7**(4), 315–320 (2010).

27. Z. G. Zhu et al., "Investigation of the permeability and optical clearing ability of different analytes in human normal and cancerous breast tissues by spectral domain OCT," *J. Biophoton.* **5**(7), 536–543 (2012).

28. A. C. Williams and B. W. Barry, "Penetration enhancers," *Adv Drug Delivery Rev.* **56**(5), 603–618 (2004).

29. M. R. Prausnitz et al., "Electroporation of mammalian skin: A mechanism to enhance transdermal drug delivery," *Proc. Natl Acad. Sci. U.S.A.* **90**(22), 10504–10508 (1993).

30. E. H. Choi et al., "The pretreatment effect of chemical skin penetration enhancers in transdermal drug delivery using iontophoresis," *Skin Pharmacol. Appl. Skin Physiol.* **12**(6), 326–335 (1999).

31. S. Henry et al., "Microfabricated microneedles: a novel approach to transdermal drug delivery," *J. Pharm. Sci.* **87**(8), 922–925 (1998).

32. S. Mitragotri, D. Blankschtein, and R. Langer, "Ultrasound mediated transdermal protein delivery," *Science* **269**(5225), 850–853 (1995).

33. H. Q. Zhong et al., "Enhancement of permeability of glycerol with ultrasound in human normal and cancer breast tissues in vitro using optical coherence tomography," *Laser Phys. Lett.* **7**(5), 388–395 (2010).

34. I. Lavon and J. Kost, "Ultrasound and transdermal drug delivery," *Drug Discovery Today* **9**(15), 670–676 (2004).

35. O. Stumpp, A. J. Welch, and T. E. Milner, "Feasibility of extracting tissue optical properties from amplitude OCT data during optical skin clearing," *Proc. SPIE* **5695**, 83–92 (2005).

36. X. Xu, R. K. Wang, and A. El Haj, "Investigation of changes in optical attenuation of bone and neuronal cells in organ culture or three-dimensional constructs in vitro with optical coherence tomography: relevance to cytochrome oxidase monitoring," *Eur. Biophys. J.* **32**(4), 355–362 (2003).

37. M. G. Ghosn, V. V. Tuchin, and K. V. Larin, "Nondestructive quantification of analyte diffusion in cornea and sclera using optical coherence tomography," *Invest. Ophthalmol. Visual Sci.* **48**(6), 2726–2733 (2007).

38. K. V. Larin et al., "Quantification of glucose diffusion in arterial tissues by using optical coherence tomography," *Laser Phys. Lett.* **4**(4), 312–317 (2007).

39. X. Xu, Q. Zhu, and C. Sun, "Assessment of the effects of ultrasound-mediated alcohols on skin optical clearing," *J. Biomed. Opt.* **14**(3), 034042 (2009).

40. G. Merino, Y. N. Kalia, and R. H. Guy, "Ultrasound-enhanced transdermal transport," *J. Pharm. Sci.* **92**(6), 1125–1137 (2003).

41. K. Tachibana et al., "Induction of cell-membrane porosity by ultrasound," *Lancet* **353**(9162), 1409 (1999).

42. J. Liu, T. N. Lewis, and M. R. Prausnitz, "Non-invasive assessment and control of ultrasound-mediated membrane permeabilization," *Pharm. Res.* **15**(6), 918–924 (1998).